

Hydrophilicity and Antibacterial Properties of Ag/TiO₂ Nanoparticle

S. Kimiagar

Islamic Azad University, Central Tehran Branch, Tehran, Iran

(Received 24 June 2013, Accepted 10 August 2013)

TiO₂ thin films and Ag/TiO₂ nanoparticles were prepared by CVD and plasma bombardment method. XRD results showed the presence of Ag nanoparticles in TiO₂ matrix. SEM image confirmed formation of Ag nanoparticles. XPS analysis was utilized to study the chemical state of the Ag/TiO₂ nanostructure. Statistical surface analysis revealed that since there is a linear relation between logarithmic diagram of Cq(r) and $r < R_c \sim 4 \mu\text{m}$ for all q, both surfaces have self-affine structure. Formation of Ag/TiO₂ nanoparticles led to the reduction of roughness of the samples from 0.72 nm to 0.61 nm. Ag/TiO₂ nanoparticles represented greater hydrophilicity under UV illumination and visible light compared with TiO₂. TiO₂ thin films and Ag/TiO₂ nanoparticles showed an inhibition for proliferation of the bacteria on their surfaces. Antibacterial activity of the samples contributed to the growth inhibition of the bacteria on their surfaces.

Keywords: Ag nanoparticles, Hydrophilicity, Antibacterial, Roughness, Self-affine

INTRODUCTION

TiO₂ as a pollution control and self-cleaning material has attracted interest in the past decades and has been widely used due to its photocatalysis and hydrophilicity properties [1]. Basically, the photocatalytic process is initiated by the photogeneration of electron/hole pairs in the semiconductor by absorption of UV-light photon. Hydrophilicity of TiO₂ surface can be induced by UV-irradiation, in this case only less than 5% of solar light energy is useful. Many efforts have been made to modify TiO₂ by impurities for improving hydrophilicity under VI light [2-4]. In order to achieve this, the reduction in the band gap energy is necessary. Many researchers have focused on doping TiO₂ with both transition metals and non-metal impurities in order to decrease the band gap. These include dye sensitization [5], semiconductor coupling [6], and impurity doping [7-9]. Modified TiO₂ by metal clusters exhibits reduction in the electron-hole recombination rate due to the Schottky barrier at the metal/TiO₂ interface.

In addition, roughness of TiO₂ thin film plays an important role in photoinduced applications because it enhances the adsorption of more molecules and produces

more efficient of thin film [10]. Hence, it is important to develop deposition method by which roughness can be controlled. Due to the importance of surface growth property, great deal of efforts have been devoted to understanding the mechanism of thin-film growth and roughness of growing surfaces in various growth methods. Analytic and numerical treatments of a simple growth model suggest that the height-height correlation function have a self-similar character and their average correlations exhibit a dynamic scaling form [11-16].

Nano particles are currently known as antibacterial materials. Among the inorganic antibacterial agents, metals and photo catalysts are most commonly used. Most metallic ions exhibit antimicrobial effect. For efficiency and safety reasons, silver, copper and zinc are the most widely available metallic antibacterial agents [17,18]. Modified TiO₂ by Ag nanoparticles is more promising for antimicrobial applications. Ag can be an efficient antibacterial material with or without light irradiation [19]. Ag doping may increase the absorption of visible light due to plasmonic effects [20].

Chemical vapor deposition (CVD) [21], sol-gel method [22], hydrothermal growth [23,24] and plasma enhanced chemical vapor deposition (PECVD) are most commonly used methods for TiO₂ films preparation. CVD is an

*Corresponding author. E-mail: kimia@khayam.ut.ac.ir

important method to fabricate uniform layer with low-porosity, high-purity, high-performance and local deposition. The process is often used to produce nano thin film and nanoparticles. This paper deals with characterization of TiO₂ films deposited by PECVD, the surface of which was subsequently modified by silver nanoparticles. The effect of these nanoparticles on hydrophilicity property, statistical surface roughness and antimicrobial properties of the nano thin films have been investigated.

EXPERIMENTAL DETAILS

Fabrication process was started by cleaning the substrate through the standard Radio Corporation of America (RCA) method (NH₄OH:H₂O₂:H₂O solution with volume ratio of 1:1:5) and then rinsed in deionized water. TiO₂ layer was deposited on glass substrate using an atmospheric pressure chemical vapor deposition (CVD) system at temperature 250 °C. TiCl₄ was used as the main precursor to form titanium dioxide. Argon gas was used for delivery of the solution from a bubbler into the chamber. Ar flow rates during the deposition were kept at 200 Sccm. Oxygen was also introduced into the chamber by a separate inlet with flow rate of 400 Sccm. In this process crystalline TiO₂ nanostructured layer was formed on the substrate. After this process 40 nm thickness of Ag layer was deposited on the TiO₂ coated substrate. The prepared samples were then placed in the DC plasma bombardment system in the presence of H₂ at a pressure of 7 Torr. Hydrogen plasma was applied on the samples with a power density of 3 W cm⁻² to form Ag nanoparticles. The properties of the coated layers are much better tunable with PECVD than in the simple thermal deposition technique, because there are more effective variable parameters.

Antibacterial activity of TiO₂ and Ag/TiO₂ was determined against E.coli using Muller Hinton agar. Agar was added to distilled water and then autoclaved. This agar plate was at 40-50 °C. In a typical preparation, Ag/TiO₂ and TiO₂ were added separately to 10⁶ of E.coli in a sterile tube. A reference tube with 10⁶ of E.coli without sample was kept at the same situation as a background in test to compare with the two sample tubes. The experiment was repeated under visible-light and in dark place. In dark conditions all

the tubes were located in dark position and the numbers of colonies were counted in agar plates after three hours and bacteria concentration was determined three times for time intervals of three hours. In the next test, all the tubes were located under 100 v lamp visible-light and after two hours, bacteria concentration was determined which repeated by time interval of two hours. All plates were incubated at 37 °C for 24 h and were tested for bacterial inhibition zones on the samples.

Phase formation and crystalline properties of the samples were characterized by an x-ray diffractometer 'XRD' (Philips PW 1130.90) in the 2θ range from 20° to 100° operating at 40 kV accelerating voltage and 40 mA current. Morphological investigation of the nanostructures was studied by a field emission scanning electron microscopy (FESEM). The components of the structure were determined by X-ray photoelectron spectroscopy (XPS) using Gamma data-scienta ESCA 200 hemispherical analyzer equipped with an Al Kα (1486.6 eV) X-ray source. The wettability of the samples was evaluated by measuring the contact angle of distilled water. The picture of water drop on the surface was captured by a digital camera and imported to the measurement software (TESCAN Measurement) to measure the angle between the distilled water curve and the sample surface. Contact angle was measured under a mercury lamp with maximum radiation at 365 nm wavelength as a UV source and halogen lamp as a visible light source. Irradiation power density of both UV and visible light was 100 mW cm⁻² at the sample position.

RESULTS AND DISCUSSION

To verify the structural characteristics of the Ag/TiO₂ nanostructure, XRD analysis was carried out. Figure 1 shows the XRD result of the prepared nanostructure. The peaks show existence of Ag in the TiO₂ matrix. Formation of Ag nanoparticles on the TiO₂ coated sample, after stopping the hydrogen bombardment, could be observed in SEM image (Fig. 2). Ag nanoparticles with a typical diameter in the range of 50-150 nm are clearly observable.

To investigate the chemical state of the Ag/TiO₂ nanostructure, XPS analysis was utilized. Figure 3 shows high-resolution XPS spectra of Ag and Ti of the prepared Ag/TiO₂. As seen from this figure, the Ag (3d_{5/2}) and Ag

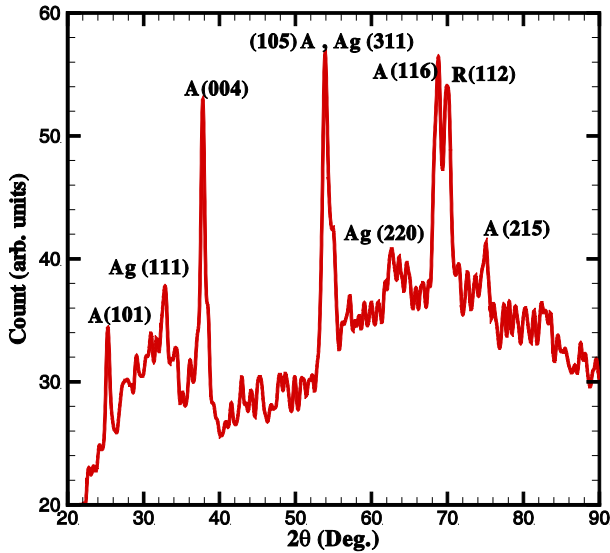


Fig. 1. XRD pattern of Ag/TiO₂ nanoparticles.

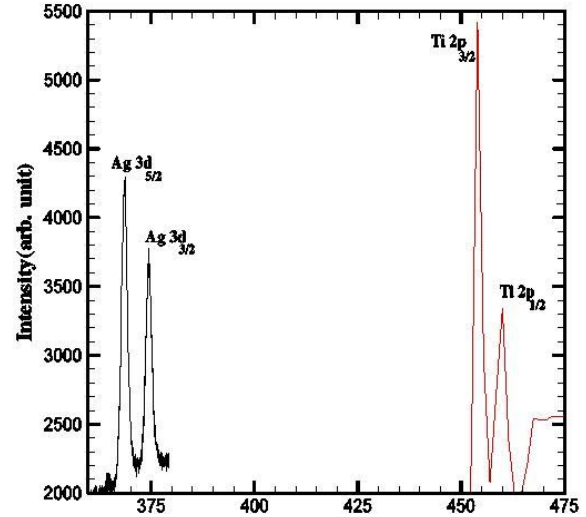


Fig. 3. XPS spectra of the Ag/TiO₂ nanoparticles.

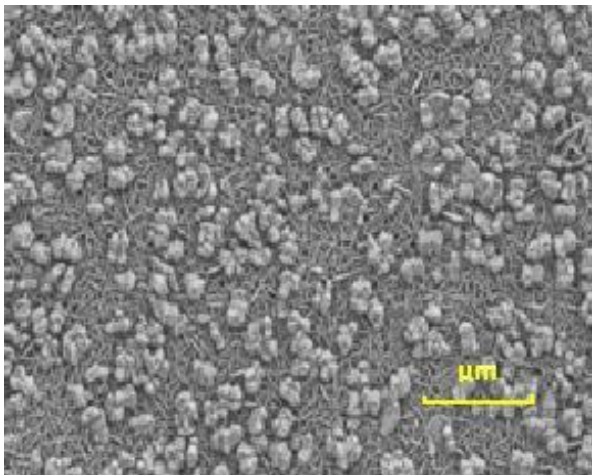


Fig. 2. SEM image of Ag/TiO₂ nanoparticles.

(3d_{3/2}) bands of the sample were found at binding energies about 368.3 and 374.1 eV, respectively.

Using statistical methods, we have investigated structure of the surfaces to find out the effect of Ag nanoparticles creation. To achieve this, we studied the scaling properties (self-affinity or multi-affinity) of the samples [10,25]. To figure out the topography of these samples, we have calculated q -th order height-height correlation function,

$$C_q(r) = \langle |h(x) - h(x+r)|^q \rangle^{1/q} \quad (1)$$

in which $h(x)$ and $h(x+r)$ are the surface heights at positions x and $x+r$ on the surface, q is order of height-height correlation function and the average is over the surface area. Generalized roughness exponent $\chi_q \sim q\zeta$ is evaluated according to the slope of the logarithmic plot of the relation $C_q(r) \sim r^{q\zeta}$ [10,25]. Figure 4 shows log-log plot of $C_q(r)$ vs. r for different values of q from $q = 2$ up to $q = 10$. In the logarithmic diagram of $C_q(r)$ vs. r there is a linear relation between $C_q(r)$ and $r < R_c$ ($R_c \sim 4 \mu\text{m}$) for all q and χ_q (the slope of the linear part in the logarithmic diagram) is the same for all q , it means that there is a self-affine structure. In the other words for self-affine structure χ_q is constant for all q , but in multi-affine structure χ_q varies for different q .

For estimating roughness exponent of these surfaces, we have calculated $C_2(r)$ using Eq. (1) and $q = 2$. The results are given in Fig. 4. Since this curve follows the scaling relation $C_2(r) \sim r^{2\zeta}$ in the length scales $r < R_c \sim 4 \mu\text{m}$, we can calculate the roughness exponent of the interfaces from the slope of the linear part of log-log curve for $q = 2$, which are 0.72 ± 0.03 nm and 0.61 ± 0.03 nm for TiO₂ and Ag/TiO₂, respectively. These exponents exhibit a meaningful change in the structure of the interfaces and can be related to its physical features [10,25,26]. It seems that the TiO₂ sample has a rough interface with larger roughness

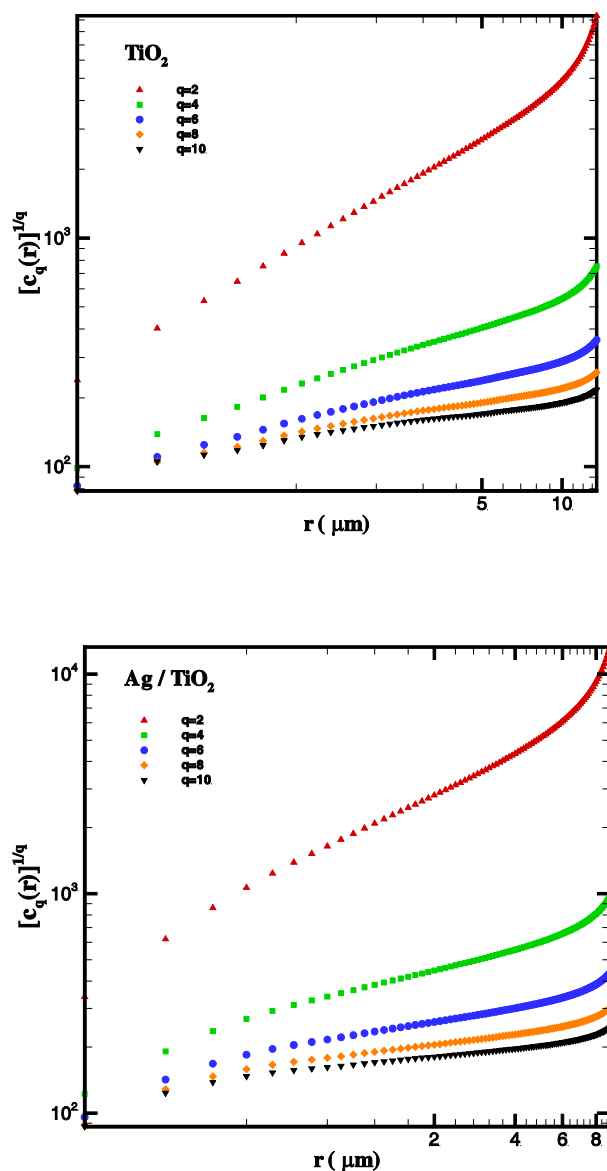


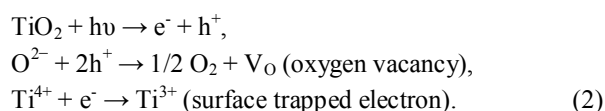
Fig. 4. log-log plot of $C_q(r)$ vs. r for different values of q , TiO₂ (left) and Ag/TiO₂ (right).

compared to the Ag/TiO₂ sample.

We can conclude from the linear feature in these diagrams that roughness exponents of the surfaces have been changed due to the creation of Ag nanoparticles, however no changes were observed on the self-affinity of the interfaces. Additionally, the higher order height-height correlation functions would represent the self-affinity of

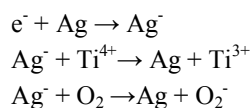
these structures.

The mechanism of photo-induced hydrophilicity of TiO₂ has been investigated by many researchers [27,28]. As a result, it was revealed that preferential adsorption of water molecules on the photo-generated defective sites of the surface lead to the formation of highly hydrophilic TiO₂ thin film surfaces [29]. Photo-generated electron-hole pairs could either recombine or move to the surface to react with species adsorbed on the surface. Some of the electrons react with lattice metal ions Ti⁴⁺ to form Ti³⁺ defective sites [30]. The formation processes of defective sites on TiO₂ surface can be expressed as follows [31]:



On the surface, trapped electrons tend to react with O₂ to form O₂⁻ or O₂²⁻ ions. Meanwhile, water molecules may change into the oxygen vacancy sites (V_O), leading to the dissociation of the water molecules on the surface [32,33]. This process increases the hydroxyl content on the TiO₂ thin film surfaces that have the ability to decompose organic and microbial matter. It was expected that the number of defective sites would increase with the increase of irradiation time and this in turn leads to the improvement of hydrophilicity.

Theoretically, the addition of noble metal to a photocatalytic semiconductor can improve the hydrophilic property. A major role of Ag incorporate in TiO₂ is to generate oxygen anion radicals (O₂⁻) and reactive center (Ti³⁺) as shown in the following reactions [34].



Therefore, increase of Ag content can increase O₂⁻ and Ti³⁺ particles which will help to prevent the electrons-holes pairs' recombination.

The water droplet was dropped onto the surface of the thin film and the contact angle was then measured from two sides and averaged as presented in Fig. 5 (inset). The lower water contact angle means more hydrophilic activity. The

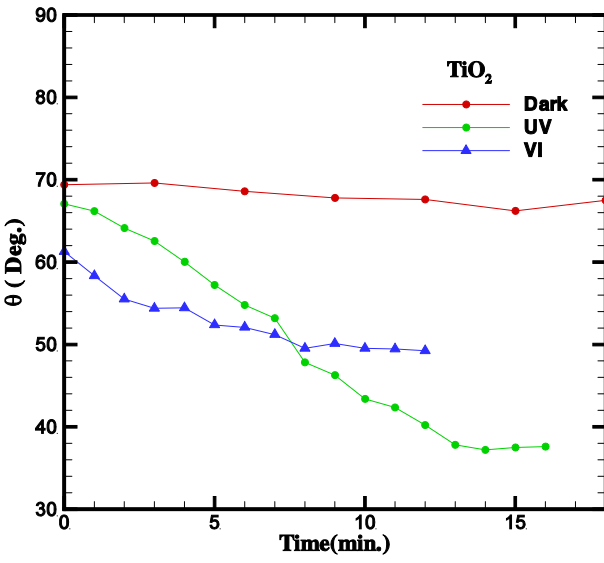
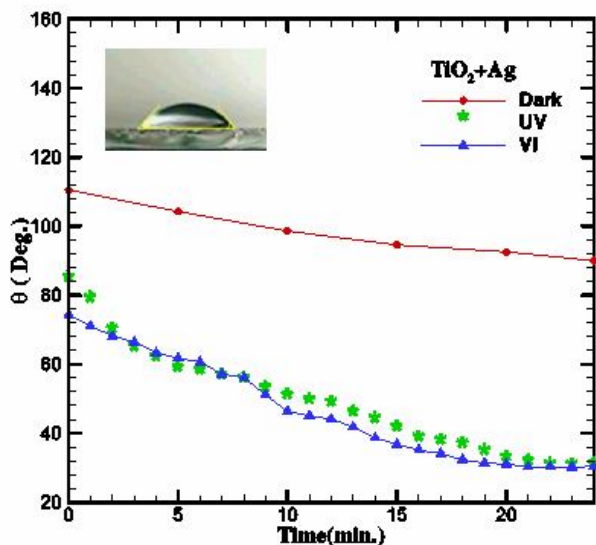


Fig. 5. Water contact angle, for Ag/TiO₂ (left) and TiO₂ (right).

contact angle of distilled water on the sample surface was measured under UV, VI illumination and also dark condition every minute. Variation of water contact angle is shown in Fig. 5. In Fig. 5-left, the Ag/TiO₂ thin film shows an angle reduction under UV and VI illumination. But for the TiO₂ thin film, Fig. 5-right, according to titanium dioxide's big band gap which cannot absorb VI light, angle reduction under VI illumination is very low. Obviously it is

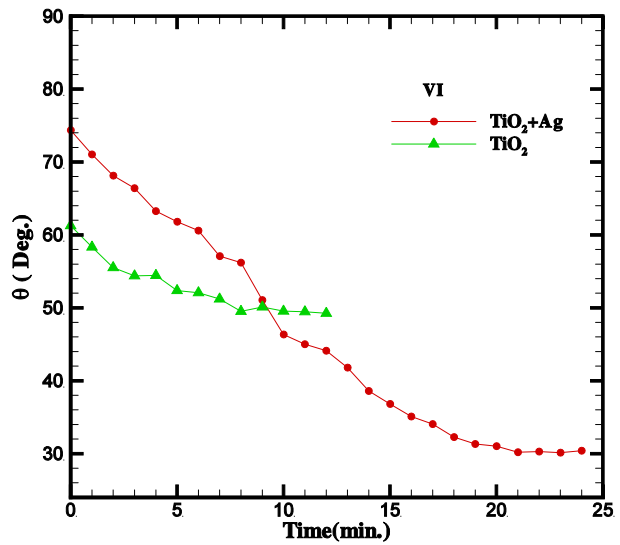


Fig. 6. Water contact angle, for Ag/TiO₂ and TiO₂ under VI light.

seen that the hydrophilicity of the TiO₂ thin film can be enhanced by Ag-doping due to the surface plasmon resonance. However, it seems that the change in the roughness exponents of the films and also different film structures could lead to a higher hydrophilicity for Ag/TiO₂ thin film. So for Ag/TiO₂ nanoparticles, improvement of hydrophilicity under VI light would be due to the band gap decrease and high surface area to volume ratio of the nanoparticles. Also increase of O₂⁻ and Ti³⁺ on the film's surface enhances the hydrophilicity of Ag/TiO₂ film. Comparison between TiO₂ and TiO₂ with Ag nanoparticles thin films is shown in Fig. 6.

Due to the outstanding application of Ag and TiO₂ in medical fields, the antibacterial efficiency of the TiO₂ and Ag/TiO₂ samples were studied under visible-light and darkness. Ag nanoparticles have a good antibacterial behavior with or without light irradiation. E. coli was loaded on samples' surface and their inactivation times were studied [16]. As a consequence, in our case, it was observed that bacteria population was affected by the samples. The results are shown in Table 1. It can be seen that TiO₂ shows weak antibacterial capability when tested in the dark place while Ag/TiO₂ has better antibacterial efficiency after three hours (Fig. 7). Compared to this, Ag/TiO₂ have a strong antibacterial efficiency under visible light during two hours

Table 1. Antibacterial Activity of Ag and Ag/TiO₂ under VI Light and Dark Place

	E.coli & TiO ₂			E.coli & Ag/TiO ₂		
	Number of bacteria	Rest of bacteria	Time (h)	Number of bacteria	Rest of bacteria	Time (h)
Dark	10 ⁶	10 ⁴	9	10 ⁶	0	9
VI-Light	10 ⁶	10 ³	8	10 ⁶	0	8

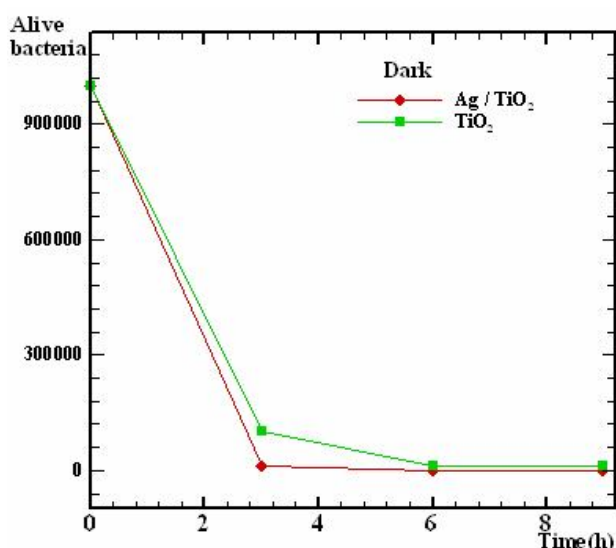


Fig. 7. Alive bacteria vs. time in a dark place for TiO₂ (square symbol) and Ag/TiO₂ (diamond symbol).

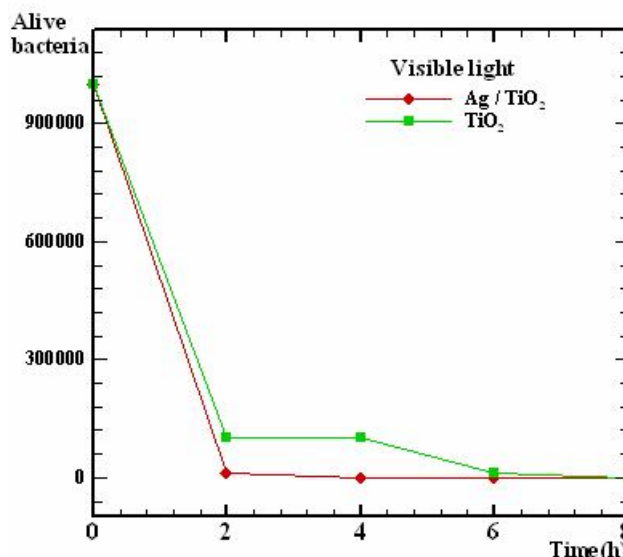


Fig. 8. Alive bacteria vs. time under visible light for TiO₂ (square symbol) and Ag / iO₂ (diamond symbol).

(Fig. 8).

CONCLUSIONS

TiO₂ thin film and Ag/TiO₂ nanoparticles were synthesized by CVD and plasma bombardment method. Base on statistical study, since there was linear relation between logarithmic diagram of $C_q(r)$ and $r < R_c \sim 4 \mu\text{m}$ for all q , surface structure was found out to be self-affine. Surface roughness of Ag/TiO₂ was lower than that of the TiO₂, so that the creation of Ag nanoparticles decreased roughness exponent of the surfaces from 0.72 nm to 0.61 nm for TiO₂ and Ag/TiO₂, respectively. The contact angle

of the water droplet was measured under UV illumination and visible light. Absorption of TiO₂ thin film was in the range of UV illumination, so contact angle decreased but under VI light there was no remarkable change in contact angle. For Ag/TiO₂ there was a reduction of contact angle under UV illumination and VI light as well, which concluded that its band gap is lower than that of the TiO₂ thin film. It means that Ag nanoparticles have improved hydrophilicity of the sample. Antibacterial experiment for the TiO₂ thin film and Ag/TiO₂ nanoparticles demonstrated that Ag/TiO₂ nanoparticles are more toxic to bacteria than TiO₂ and it can make E. coli inactive after two hours. This result showed the capability of green reduction of Ag/TiO₂

that can be applied for inhibition of the bacterial growth on surfaces, even in the environments which are highly suitable for proliferation of the bacteria.

This work shows the possibility of creation nanoparticles with plasma bombardment. Since there are many parameters for plasma that are adjustable, it is conceivable to optimize the nanoparticle size by considering the effect of parameters such as temperature, pressure and time of bombardment, synthesis method and plasma voltage to have nanoparticles with required size, band gap, surfaces with specified roughness and with specific physico-chemical properties. The effect of nanoparticle size on optical property, antibacterial activity and efficiency enhancement of dye-sensitized solar cells has already been reported [35-38]. Hence, our method presents more parameters to control size of the nanoparticle to improve the properties and to formulate new products with many biotechnological applications. Compared with other conventional methods, the proposed method in this study has some advantages due to the ability of parameter adjustment.

REFERENCES

- [1] K. Guan, *Surf. Coat. Technol.* 191 (2005) 155.
- [2] M. Vohra, S. Kim, W. Choi, *J. Photochem. Photobiol. A Chem.* 160 (2003) 55.
- [3] S. Hata, Y. Kai, I. Yamanaka, *et al.*, *JSAE Rev.* 21 (2000) 97.
- [4] R. Asahi, T. Morikawa, T. Ohwahi, *et al.*, *Science* 293 (2001) 269.
- [5] J. Moon, C.Y. Yun, K.W. Chung, M.S. Kang, J. Yi, *Catal. Today* 87 (2003) 77.
- [6] S. Kim, W. Choi, *J. Phys. Chem. B* 109 (2005) 5143.
- [7] F.B. Li, X.Z. Li, *Chemosphere* 48 (2002) 1103.
- [8] Y.L. Kuo, H.W. Chen, Young Ku, *Thin Solid Films* 515 (2007) 3461.
- [9] S.Y. Treschev, P.W. Chou, Y.H. Tseng, J.B. Wang, E.V. Perevedentseva, C.L. Cheng, *Appl. Catal. B: Environ.* 79 (2008) 8.
- [10] O. Zywitzki, T. Modes, P. Frach, D. Gloss, *Surf. Coat. Technol.* 202 (2008) 2488.
- [11] A.L. Barabasi, H.E. Stanley, *Fractal Concepts in Surface Growth*, New York, Cambridge University Press, 1995.
- [12] T. Halpin-Healy, Y.C. Zhang, *Phys. Rep.* 245 (1995) 215.
- [13] J. Krug, H. Spohn, in: C. Godreche (Ed.), *Solids Far from Equilibrium Growth, Morphology and Defects* New York, Cambridge University Press, 1990.
- [14] P. Meakin, *Fractal, Scaling and Growth Far from Equilibrium*, Cambridge: Cambridge University Press, 1998.
- [15] M. Kardar, *Physica A* 281 (2000) 295.
- [16] A.A. Masoudi, F. Shahbazi, J. Davoudi, M.R. Rahimi Tabar, *Phys. Rev. E* 65 (2002) 026132.
- [17] O. Akhavan *J. Colloid Interface Sci.* 336 (2009) 117.
- [18] J. Chen, G. Wan, Y. Leng, *et al.* *Sci. China Ser E- Technol. Sci.* 49 (2006) 20.
- [19] E.V. Skorb, L.I. Antonouskaya, N.A. Belyasova, D.G. Shchukin, H. Mohwald, D.V. Sviridov, *Appl. Catal. B- Environ.* 84 (2008) 94.
- [20] K. Awazu, M. Fujimaki, C. Rockstuhl, J. Tominaga, H. Murakami, Y. Ohki, N. Yoshida, T. Watanabe, *J. Am. Chem. Soc.* 130 (2008) 1676.
- [21] S.K. Pradhan, P.J. Reucroft, F. Yang, A. Dozier, *J. Cryst. Growth* 256 (2003) 83.
- [22] T. Sugimoto, K. Okada, H. Itoh, *J. Colloid Interface Sci.* 193 (1997) 140.
- [23] M. Wu, G. Lin, D. Chen, G. Wang, D. He, S. Feng, R. Xu, *Chem. Mater.* 14 (2002) 1974.
- [24] S. Yang, L. Gao, *J. Am. Ceram. Soc.* 2488 (2005) 968.
- [25] A.I. Zad, G. Kavei, M.R. Rahimi Tabar, S.M.V. Allaei, *J. Phys. Condens. Matter* 15 (2003) 1889.
- [26] P. Sangpour, G.R. Jafari, O. Akhavan, A.Z. Moshfegh, M.R. Rahimi Tabar, *Phys. Rev. B* 71 (2005) 155423.
- [27] N. Sakai, A. Fujishima, T. Watanabe, K. Hashimoto, *J. Phys. Chem. B* 105 (2001) 3023.
- [28] R. Wang, N. Sakai, A. Fujishima, T. Watanabe, K. Hashimoto, *Phys. Chem. B* 103 (1999) 2188.
- [29] M.R. Hoffmann, S.T. Martin, W. Choi, D.W. Bahnemann, *Chem. Rev.* 95 1 (1995) 69.
- [30] S.D. Sharma, D. Singh, K.K. Saini *et al.*, *Appl. Catal. A* 314 (2006) 40.
- [31] J.C. Yu, J. Yu, W. Ho, J. Zhao, *Photochem. Photobiol. A Chem.* 148 (2002) 331.
- [32] R. Wang, K. Hashimoto, A. Fujishima *et al.*, *Adv. Mater.* 10 (1998) 135.

- [33] R.D. Sun, A. Nakajima, A. Fujishima, T. Watanabe, K. Hashimoto, *Phys. Chem. B* 105 (2001) 1984.
- [34] J. Kirchnerova, M.L.H. Cohen, C. Guy, D. Klvana, *Appl. Catal. A-General*. 282 (2005) 321.
- [35] L. Bedel, C. Cayron, M. Jouve, F. Maury, *Nanotechnology* 23 (2012) 015603.
- [36] C. Photiphitak, P. Rakkwamsuk, P. Muthitamongkol, C. Sae-Kung, C. Thanachayanont, *Int. J. Photoenergy* 2011 (2011) 1.
- [37] L. Mai, D. Wang, S. Zhang, Y. Xie, C. Huang, Z. Zhang, *Appl. Surf. Sci.* 257 (2010) 974.
- [38] M. Guzman, J. Dille, S. Godet, *Nanomed. Nanotechnol. Biol. Med.* 8 (2012) 37.